

Modeling Imatinib-Treated Chronic Myelogenous Leukemia

Cara Peters

cpeters3@math.umd.edu

Advisor: Dr. Doron Levy

dlevy@math.umd.edu

Department of Mathematics

Center for Scientific Computing and Mathematical Modeling

Abstract

Chronic Myelogenous Leukemia (CML) is a blood cancer affecting approximately 1 in 100,000 people. While there are many different treatments for controlling CML, there is currently no cure. Recently, many mathematical models have been developed to explore disease genesis and the effects of various therapies with the hope of improving or discovering new therapeutic strategies. In this project three such models are studied: an agent-based model, a system of difference equations, and a system of partial differential equations.

1 Project Background

Chronic Myelogenous Leukemia (CML) is a type of blood cancer resulting in the overproduction of white blood cells. Approximately 20% of all leukemia cases are CML. CML can be characterized by a genetic mutation in hematopoietic stem cells in which a translocation between chromosomes 9 and 22 occurs. During this translocation, fusion of the bcr-abl gene occurs on chromosome 22 to form what is known as the Philadelphia (Ph) chromosome, a detectable characteristic in 90% of all CML patients. Fusion of this gene results in increased tyrosine kinase activity contributing to uncontrolled stem cell growth and survival, and ultimately cancer.

There are currently many types of treatment available to CML patients. Of particular interest is a form of targeted therapy involving the drug Imatinib. Imatinib is a tyrosine kinase inhibitor that specifically targets Ph⁺ cells and binds to the bcr-abl enzyme. This drug controls the population of cancer cells in two ways: by preventing proliferation of mutated cells and increasing apoptosis or cellular suicide. Although quite effective as a control, Imatinib is not a cure for CML.

In the past decade, there has been much interest in the use of mathematical models to gain further insight into the dynamics of CML genesis and explore the effects of treatment. This project will consider three such models, each biologically based on the same cell differentiation process as described by Roeder *et al.* This process consists of three stages of cell differentiation: stem cells, precursors and mature cells. Additionally, stem cells are categorized as either non-proliferating (A) or proliferating cells (Ω). Movement between compartments is as follows (fig. 1).

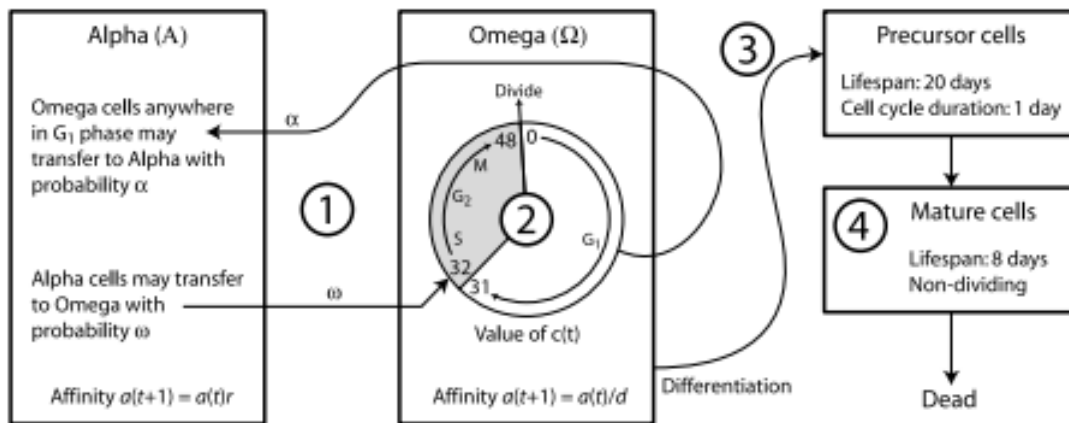


Figure 1: A cell state diagram as proposed by Roeder *et al.* Figure from [2].

Each stem cell may be characterized by its cellular affinity, a quantity based on cell age and state. Cells in A increase their affinity over time until the maximum affinity is reached. They transfer from A to Ω with probability ω determined by affinity and the total number of proliferating cells. In Ω , stem cells proliferate by completing the 48 hour cell cycle. The cell cycle consists of four necessary phases for cell growth and division. These stages in order are G₁, S, G₂, and M. Cells enter Ω from A at hour 32 of the cell cycle, the beginning of the S phase during which DNA synthesis occurs. At hour 48, the cell divides into two identical daughter cells

that each begin the cycle in the G_1 growth phase. Transitions from Ω to A occur during the G_1 phase with probability α . Cell affinity decreases over time in Ω until the minimum affinity is attained.

Stem cells with minimum affinity differentiate into precursor cells. These cells divide symmetrically once every 24 hours for 20 days, at which point they become mature cells. Cells live in the mature stage for 8 days before dying.

The biology described here is a simplification of the cell maturation process and makes a few assumptions. Firstly, the differentiation process has been reduced to three stages of maturation. Second, transition probabilities between stem cell compartments are assumed to be based on affinity, an internal quantity for each stem cell that varies in time within an interval $[a_{\min}, a_{\max}]$. Affinity is a notion whose existence was postulated by Roeder [1] and is not directly associated with any known biological mechanism specific to the hematopoietic system. Furthermore, the time spent in each stage is deterministic. It is assumed that these lifespans are known and fixed. Lastly, it is assumed that when a cell undergoes mitosis and divides, it does so symmetrically. This means that each daughter cell is identical and of the same type of cell as the parent, i.e. stem cells divide into two stem cells, precursors divide into two precursors.

2 Approach

There are three components to this project. The first is an agent based model (ABM) for simulating CML genesis as described by Roeder *et al.* The second component is an implementation of a reformulation of the ABM model as a system of discretized difference equations [2]. Lastly, a system of PDEs is used to simulate CML and its treatment [3]. All three algorithms are based upon the same underlying biological model (fig. 1) and use the same parameter values as given by Roeder (table B.1). Three cell populations will be simulated: healthy, leukemic and Imatinib-affected leukemic. These populations will be denoted Ph^- , Ph^+ and $Ph^{+/A}$, respectively, where Ph represents the presence of the Philadelphia chromosome.

2.1 Agent Based Model

Roeder's agent based model simulates each cell individually according to a set of rules (fig. 2). At each discrete time step these rules are applied and cells are updated simultaneously. At the start of each time step, the number of cells in the A and Ω compartments is determined and used to govern the movement of each stem cell in the model. As previously mentioned, cells in A transition to Ω with probability ω , while cells in Ω move to A with probability α .

$$\begin{aligned}\omega(\Omega(t), a(t)) &= \frac{a_{\min}}{a(t)} f_{\omega}(\Omega(t)) \\ \alpha(\Omega(t), a(t)) &= \frac{a(t)}{a_{\max}} f_{\alpha}(A(t))\end{aligned}\tag{1}$$

The transition probabilities are dependent on the affinity $a(t)$ as well as the number of non-proliferating cells $A(t)$ and proliferating cells $\Omega(t)$. The functions f_ω and f_α are sigmoidal functions, which are given by equation (B.1) in the appendix.



Figure 2: Update algorithm for ABM stem cells. Cell affinity is given by $a(t)$, position in cell cycle by $c(t)$ and cell compartment by $m(t)$. $\Delta t = 1 \text{ hr}$. From [1].

Cells that remain in A increase affinity by a factor r known as the regeneration factor. When cells transfer into Ω , $c(t)$ is set to 32 to correspond to the beginning of the S phase of the cell cycle. Cells remaining in Ω , may only transition to A when $c(t)$ corresponds to the G_1 phase ($0 \leq c(t) \leq 31$). Once the cell cycle has been completed, the cell duplicates. Affinity of Ω cells is decreased by a differentiation factor $1/d$ until minimum affinity is reached. A cell with minimum affinity begins terminal differentiation. Unlike the stem cells in this model, the behavior of the differentiated cells is not stochastic. Precursor and mature cells move according to fixed rules, as given by the cell state diagram (fig. 1).

2.1.1 Simulation of CML Genesis

The algorithm depicted in figure 2 demonstrates the rules for updating healthy or Ph^- cells. To simulate the onset of CML in a healthy patient and track disease genesis, parameters of the sigmoidal functions f_ω and f_α of a single cell are set to values specific to leukemic cells. That cell will be labeled leukemic (Ph^+) and tracked over time. All of its progeny will be considered as Ph^+ cells.

2.1.2 Simulation of Treatment

Treatment is introduced to the algorithm in two ways, reflecting the two ways Imatinib can affect Ph^+ cells. First, Imatinib can limit proliferation of mutated cells. This will be accomplished in the model by altering the f_ω function for previously unaffected Ph^+ cells, with probability r_{inh} at each time step. Once this change has been made, these cells will be marked as affected ($\text{Ph}^{+/A}$) and maintain this configuration of ω for the duration of the simulation. Altering this function alone decreases the ability for resting cells to transition to Ω and begin proliferating. Imatinib also increases apoptotic activity in Ph^+ cells, causing cells to die. Implementation of this function will consist of removing Ph^+ and $\text{Ph}^{+/A}$ cells in Ω from the system, with probability r_{deg} , at each time step.

Simulation of Imatinib treatment will begin once the proportion of differentiated Ph^+ cells has reached more than 99.5% of the total cell population. To stop treatment, all parameter values and functions are reset to their initial values.

2.2 A System of Difference Equations Model

Model 2 formulates the cell state diagram as a system of discretized difference equations. Rather than simulating each cell individually as the ABM model does, this system groups cells by their common characteristics i.e., cell state compartment, affinity level, cell cycle position. The progression of CML is simulated by tracking the number of cells in each group. This approach reduces computational complexity and allows for simulation of realistic cell numbers.

In order to devise the difference equations, the state space must be discretized. Time is already discretized in the ABM; cell positions are updated at fixed and uniform time steps. Affinity is discretized by setting $a(t) = e^{-k\rho}$ where $\rho = \log(d) \approx 0.0488$ and $0 \leq k \leq 127$ is an integer. The affinity of each cell can now be characterized discretely by the value of k where $\log(a(t)) = -k\rho$.

2.2.1 The Difference Equations

The stem cell populations can be represented by the following difference equations with k representing cell affinity and c representing position in the cell cycle:

$$A_k(t+1) = \begin{cases} (A_0(t) - B_0(t)) + (A_1(t) - B_1(t)) + (A_2(t) - B_2(t)), & k = 0 \\ (A_{k+2}(t) - B_{k+2}(t)) + \sum_{c=0}^{31} \Psi_{k,c}(t), & k = 1, \dots, 125 \\ \sum_{c=0}^{31} \Psi_{k,c}(t), & k = 126, 127 \end{cases} \quad (2)$$

$$\Omega_k(t+1) = \begin{cases} B_0(t), & k = 0, c = 32 \\ 2\Omega_{k-1,48}(t), & k > 0, c = 0 \\ \Omega_{k-1,c-1}(t) - \Psi_{k-1,c-1}(t), & k > 0, c = 1, \dots, 31 \\ (\Omega_{k-1,31}(t) - \Psi_{k-1,31}(t)) + B_k(t), & k > 0, c = 32 \\ \Omega_{k-1,c-1}(t), & k > 0, c = 33, \dots, 48 \\ 0 & \text{otherwise} \end{cases} \quad (3)$$

Transitions between the A_k and $\Omega_{k,c}$ compartments are determined by the binomial random variables B_k and $\Psi_{k,c}$ which have the following distributions:

$$B_k(t) \sim \text{Bin}(A_k(t), \omega(\Omega(t), e^{-k\rho}))$$

$$\Psi_{k,c}(t) \sim \text{Bin}(\Omega_{k,c}(t), \alpha(A(t), e^{-k\rho})), \quad c = 0, \dots, 31$$

Here $\Omega(t) = \sum_{k,c} \Omega_{k,c}(t)$ and $A(t) = \sum_k A_k(t)$ denote the total number of proliferating and resting cells respectively. The transition probabilities ω and α are as previously given by (1).

The differentiated cells can be represented in a similar fashion. The equations for precursors are denoted by $P_j(t)$ where $j = 0, \dots, 479$ is the number of hours a cell has spent in this compartment, up to 20 days. Similarly mature cells are denoted by $M_j(t)$ where $j = 0, \dots, 191$ is the number of hours spent as a mature cell, up to 8 days.

$$P_j(t+1) = \begin{cases} \sum_{c=0}^{48} \Omega_{127,c}(t) - \sum_{c=0}^{31} \Psi_{127,c}(t), & j = 0 \\ 2P_{j-1}(t), & j = 24, 48, 72, \dots, 456 \\ P_{j-1}(t), & \text{otherwise} \end{cases} \quad (4)$$

$$M_j(t+1) = \begin{cases} 2P_{479}(t), & j = 0 \\ M_{j-1}(t), & \text{otherwise} \end{cases} \quad (5)$$

These equations directly reflect the rules of cell differentiation as presented in the cell state diagram (fig. 1). The first line of (4) represents proliferating cells that have attained minimum affinity and differentiate into precursors. Precursors divide every 24 hours, producing two daughter cells, as represented by line two. Line three denotes an increase in age, which is necessary to track the time spent as a precursor before maturing. The first line of (5) signifies the number of precursors that undergo one final division before entering the mature state. Similar to the final line of (4), the second line of (5) tracks the age of mature cells before they die.

2.2.2 Modeling CML and Imatinib Treatment

Three non-interacting cell populations are simulated to mathematically model clinically observed phenomena. These populations are healthy cells (Ph^-), leukemic cells (Ph^+) and Imatinib-affected cells ($\text{Ph}^{+/A}$). Equations (2) to (5) as written were used to simulate Ph^- cells. Alterations to equation (3) and new parameter values were used to represent Ph^+ and $\text{Ph}^{+/A}$ cells.

Ph^+ cells uncontrollably proliferate, therefore the transition rates between A and Ω differ from those of Ph^- cells. The transition functions $f_{\alpha/\omega}$ are updated with new parameter values (see table B.1) that correspond to this behavior. This is the only update necessary to simulate CML genesis. Equations (2) – (5) remain unchanged.

A slight alteration to equation (3) for Ph^+ Ω cells is made when treatment simulation begins; equations (2), (4) and (5) are as previously stated. When Imatinib is introduced, proliferating stem cells become Imatinib affected with probability r_{inh} and undergo apoptosis with probability r_{deg} at each time step. The number of proliferating Ph^+ stem cells infected at time t is given by $\Omega^{+/I}(t) \sim \text{Bin}(\Omega_{k,c}^+(t), r_{inh})$. The number of proliferating stem cells that die at time t is given by $\Omega^{+/D}(t) \sim \text{Bin}(\Omega_{k,c}^+(t), r_{deg})$. These cells are removed from the Ph^+ cell population at the beginning of each time step before any other transition occurs. To accomplish this, $\Omega_{k,c}^{+/R}(t)$ is substituted into the right hand side of (3), where $\Omega_{k,c}^{+/R}(t) = \Omega_{k,c}^+(t) - \Omega_{k,c}^{+/I}(t) - \Omega_{k,c}^{+/D}(t)$ is the number of cycling Ph^+ stem cells remaining unaffected for the next time step. The overall structure of the equations remains unchanged.

The $\text{Ph}^{+/A}$ cell population differs from Ph^- cells in two ways. First, since Imatinib inhibits the ability of these cells to proliferate, transition functions $f_{\alpha/\omega}$ will be updated with corresponding parameter values (table B.1). Second, affected proliferating stem cells, $\Omega^{+/A}$ undergo apoptosis at each time step according to a binomial distribution with probability r_{deg} . These cells are removed at the beginning of each time step and infected cells are added, before regular transitions occur. In terms of the equations, $\Omega^{+/A,R}(t)$ is substituted into the right hand side of (3) where $\Omega^{+/A,R}(t) = \Omega_{k,c}^{+/A}(t) - \Omega_{k,c}^{+/A,D}(t) + \Omega_{k,c}^{+/I}(t)$. This new quantity is used to calculate $\Omega_{k,c}^{+/A}(t+1)$. Again, equations (2), (4) and (5) and the overall structure of (3) remain unchanged for $\text{Ph}^{+/A}$ population.

2.3 A PDE Model

The third model transforms Roeder's ABM into a system of partial differential equations, the goal being to describe the same CML dynamics but with continuous variables. The PDE model has advantages over the original model. Like the system of difference equations, it is designed to reduce the complexity of the ABM, which can produce a solution in less time and allows simulations of realistic cell population sizes. Additionally, it tracks disease genesis in continuous time which more accurately reflects true biological processes.

Transitions for stem cells will be governed by three variables t , a and c , which can be thought of as three internal clocks representing real time, affinity and cell cycle position

respectively. Differentiated cells are not dependent on affinity or the cell cycle. Lifespans and functions of these cells will be represented by t and s , where s denotes cell age.

2.3.1 The System and Boundary Conditions

As noted in the difference equation model, the log of cell affinity is linear with respect to real time. Hence, the population of non-proliferating cells A will be denoted $A(x, t)$ where $x = -\log(a)$ with a being affinity. Over time, cells in A increase their affinity up to some maximum value. This will correspond to $x_{min} = -\log(a_{max})$. To deal with the accumulation of cells occurring at this boundary, cells with maximum affinity will be considered as a subpopulation denoted $A^*(t)$. The population of proliferating cells will be denoted $\Omega(x, c, t)$. Additionally, $\Omega^*(x, t)$ will be used to denote the subpopulation of proliferating cells that transferred from A^* .

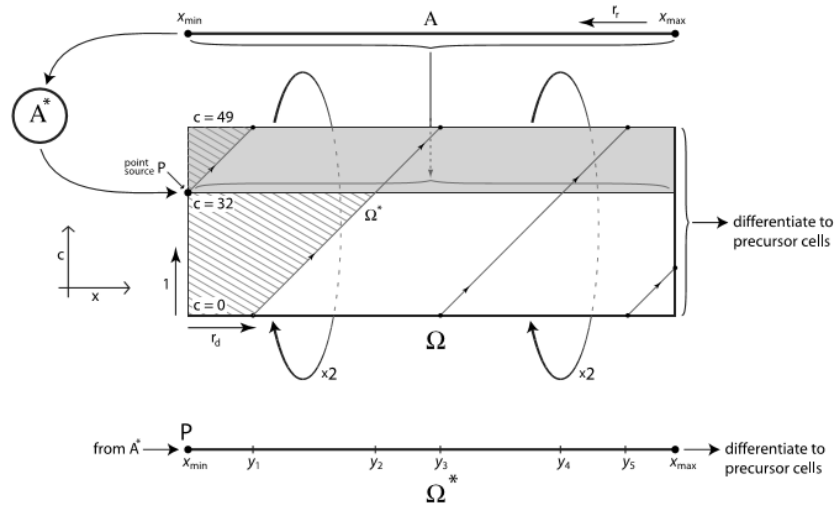


Figure 3: A representation of the stem cell compartments for the PDE model. Alpha stem cells decrease their log affinity until reaching a minimum value, at which point they are shifted to the A^* compartment. Omega stem cells increase their log affinity values x and position in the cell cycle c . The shaded region corresponds to the portion of the cell cycle during which cells prepare for and undergo mitosis. The unshaded region corresponds to the G_1 growth phase during which cells can transfer to Alpha. Cells that transfer from Alpha enter Omega at the line denoted $c=32$. A^* becomes a point source for the population of Ω^* cells. These cells increase their log affinity values over time and complete specific phases of the cell cycle at the time counters $y_1, y_2, y_3, y_4,$ and y_5 . From [3].

The PDEs for these four subpopulations are as follows:

$$\frac{\partial A}{\partial t} - \rho_r \frac{\partial A}{\partial t} = -\omega(\bar{\Omega}, e^{-x})A + \alpha(\bar{A}, e^{-x}) \int_0^{32} \Omega(x, c, t) dc + \begin{cases} 0, & x \in X_a \\ \alpha(\bar{A}, e^{-x})\Omega^*, & x \in X_b \end{cases} \quad (6)$$

$$\frac{dA^*}{dt} = \rho_r A(x_{min}, t) - \omega(\bar{\Omega}, e^{-x_{min}})A^* \quad (7)$$

$$\frac{\partial \Omega}{\partial t} + \rho_d \frac{\partial \Omega}{\partial x} + \frac{\partial \Omega}{\partial c} = \begin{cases} -\alpha(\bar{A}, e^{-x})\Omega, & \text{for } c \in (0, 32] \\ 0, & \text{for } c \in (32, 49] \end{cases} \quad (8)$$

$$\frac{\partial \Omega^*}{\partial t} + \rho_d \frac{\partial \Omega^*}{\partial x} = \begin{cases} 0, & x \in X_a \\ -\alpha(\bar{A}, e^{-x})\Omega^*, & x \in X_b \end{cases} \quad (9)$$

The domain of x is divided into two subsets X_a and X_b where $X_a = (x_{min}, y_1] \cup (y_2, y_3] \cup (y_4, y_5]$ and $X_b = (y_1, y_2] \cup (y_3, y_4] \cup (y_5, x_{max}]$, with y_1, y_2, y_3, y_4 , and y_5 being constants corresponding to affinity values at which Ω^* cells reach cell cycle time counters of 49, 32, 49, 32, and 49 respectively [3]. The transition probabilities ω and α are given by (1). Regeneration and differentiation factors for affinity are incorporated into the advection rates $\rho_r = \log r$ and $\rho_d = \log d$. Equations (6) - (9) are dependent on the total population of cells in A and Ω . These are denoted by

$$\bar{A}(t) = \int_{x_{min}}^{x_{max}} A(x, t) dx + A^*(t)$$

$$\bar{\Omega}(t) = \int_{x_{min}}^{x_{max}} \int_0^{49} \Omega(x, c, t) dc dx + \int_{x_{min}}^{x_{max}} \Omega^*(x, t) dx$$

Boundary conditions for A and Ω are given by

$$\begin{aligned} A(x_{min}, t) &= 0 \\ \Omega(x, 0, t) &= 2\Omega(x, 49, t) \\ \Omega(x, 32^+, t) &= \Omega(x, 32^-, t) + \omega(\bar{\Omega}, e^{-x})A \\ \Omega^*(x_{min}, t) &= \frac{\omega(\bar{\Omega}, e^{-x_{min}})}{\rho_d} A^* \\ \Omega(y_i^+, t) &= 2\Omega(y_i^-, t), \quad i = 1, 3, 5 \end{aligned} \quad (10)$$

Cells that have attained minimum affinity differentiate into precursor cells, where their behavior is no longer dependent on affinity or the cell cycle seen in Ω . The PDE for these cells can then be written as a linear advection equation based on age:

$$\frac{\partial P}{\partial t} + \frac{\partial P}{\partial s} = 0, \quad s \in [0, 480) \quad (11)$$

Precursors divide once every 24 hours. This will be incorporated into the boundary conditions for (11) which are given as

$$\begin{cases} P(0, t) = \rho_d \left(\int_0^{32} \Omega(x_{max}, c, t) dc + \Omega^*(x_{max}, t) \right) \\ P(v^+, t) = 2P(v^-, t), \quad v = 24, 48, 72, \dots, 456 \end{cases} \quad (12)$$

Here, the boundaries are considered to be the times at which division occurs. Mature cells can be considered in a similar fashion, as their population depends only on real time and cell age. The PDE is given by (13) with boundary condition (14) to signify the final division of precursor cells.

$$\frac{\partial M}{\partial t} + \frac{\partial M}{\partial s} = 0, \quad s \in [0,192) \quad (13)$$

$$M(0, t) = 2P(480, t) \quad (14)$$

2.3.2 Modeling CML and Imatinib Treatment

Simulating disease genesis and treatment in the PDE model will be similar as in the difference equations. Leukemic cells will be denoted by Ph^+ , nonleukemic cells as Ph^- and Imatinib-affected leukemic cells by $\text{Ph}^{+/A}$. A separate set of PDEs will be formulated for each population according to equations (6) - (9), (11) and (13), with some modifications for Ph^+ and $\text{Ph}^{+/A}$ cells. The boundary conditions will remain the same across all populations. PDEs for Ph^- cells are as written above.

Unaffected Ph^+ cells transition between A and Ω based on transition functions $f_{\alpha/\omega}$, with parameter values specific to Ph^+ cells (table B.1). Proliferating leukemic cells Ω^+ can become Imatinib affected or undergo apoptosis. This is introduced in by altering (8) and (9) to include an additional term on the right hand side: $-(r_{inh} + r_{deg})\Omega^+$ and $-(r_{inh} + r_{deg})\Omega^{*,+}$ respectively. The rest of the PDEs and boundary conditions remain unchanged.

Imatinib-affected cells transition between A and Ω based on transition functions $f_{\alpha/\omega}$, with parameter values specific to $\text{Ph}^{+/A}$ cells (table B.1). The effects of Imatinib are introduced by including an additional right hand side term to (8) and (9) of the form $r_{inh}\Omega^+ - r_{deg}\Omega^i$ and $r_{inh}\Omega^{*,+} - r_{deg}\Omega^{*,i}$ respectively. Here Ω^i denotes the affected proliferating stem cell population. Again, all other equations for the $\text{Ph}^{+/A}$ cells are as given by (6), (7), (11) and (13). The boundary conditions remain unchanged.

2.3.3 Numerical Methods

To numerically simulate the PDE model, first the domain will be discretized into an equally spaced grid. The equations and boundary conditions given above will be discretized using the numerical scheme presented by Kim *et al.* Starting with the stem cells, the grid points for the domain $[x_{min}, x_{max}] \times [0, 49] \times \mathbb{R}_0^+$ are given by $x_j = j\Delta x$, $c_k = k\Delta c$ and $t_n = n\Delta t$, where

$$\Delta x = \frac{x_{max} - x_{min}}{J}, \quad \Delta c = \frac{49}{K}$$

and $j = 0, \dots, J$, $k = 0, \dots, K$, and $n = 0, \dots, N$. Let $\lambda_x = \Delta t/\Delta x$ and $\lambda_c = \Delta t/\Delta c$ be the fixed mesh ratios. The composite trapezoidal rule will be used to evaluate all integrals that appear in the above equations and is denoted by $\mathcal{J}_u(f) = \frac{\Delta u}{2} \sum_{l=0}^{M-1} (f(u_{l+1}) - f(u_l))$. Note that $\widehat{A}_n, \widehat{\Omega}_n, \widetilde{A}_{j,n}, \widetilde{A}_n^*, \widetilde{\Omega}_{j,k,n}$ and $\widetilde{\Omega}_{j,n}^*$ will represent the numerical approximations for $\overline{A}(t_n), \overline{\Omega}(t_n), A(x_j, t_n), A^*(t_n), \Omega(x_j, c_k, t_n)$ and $\Omega^*(x_j, t_n)$ respectively. Following this notation,

$$\widehat{A}_n = \mathcal{J}_x(\widetilde{A}_{-,n}) + \widetilde{A}_n^*,$$

$$\widehat{\Omega}_n = \mathcal{T}_x \circ \mathcal{T}_c(\widetilde{\Omega}_{-, -, n}) + \mathcal{T}_x(\widetilde{\Omega}_{-, n}^*)$$

Then the numerical approximation for (6) is

$$\begin{aligned} \widetilde{A}_{j, n+1} = \widetilde{A}_{j, n} + \lambda_x \rho_r (\widetilde{A}_{j+1, n} - \widetilde{A}_{j, n}) - \Delta t (\omega(\widehat{\Omega}_n, e^{-x_j}) \widetilde{A}_{j, n} - \alpha(\widehat{A}_n, e^{-x_j}) \mathcal{T}_c(\widetilde{\Omega}_{j, -, n})) \\ + \begin{cases} 0, & x_j \in X_a, \\ (\Delta t) \alpha(\widehat{A}_n, e^{-x_j}) \widetilde{\Omega}_{j, n}^*, & x_j \in X_b. \end{cases} \end{aligned}$$

with associated boundary condition obtained from the first line of (10)

$$\widetilde{A}_{j, n+1} = 0.$$

The approximation for (7) is given as

$$\widetilde{A}_{n+1}^* = \widetilde{A}_n^* + \Delta t \left(\rho_r A_{0, n} - \frac{\omega(\widehat{\Omega}_n, e^{-x_0})}{\rho_d} \widetilde{A}_n^* \right).$$

The numerical scheme for Ω cells is derived from (8) as

$$\begin{aligned} \widetilde{\Omega}_{j, k, n+1} = \widetilde{\Omega}_{j, k, n} + \lambda_x \rho_d (\widetilde{\Omega}_{j, k, n} - \widetilde{\Omega}_{j-1, k, n}) - \lambda_c (\widetilde{\Omega}_{j, k, n} - \widetilde{\Omega}_{j, k-1, n}) \\ + \begin{cases} -(\Delta t) \alpha(\widehat{A}_n, e^{-x_j}) \Omega_{j, k, n}, & \text{for } c \in (0, 32], \\ 0, & \text{for } c \in (32, 49]. \end{cases} \end{aligned}$$

with boundary conditions

$$\begin{aligned} \widetilde{\Omega}_{0, k, n} &= 0 \quad \forall k, n \\ \widetilde{\Omega}_{j, 0, n+1} &= 2\widetilde{\Omega}_{j, K, n} \\ \widetilde{\Omega}_{j, \overline{k}^+, n+1} &= \widetilde{\Omega}_{j, \overline{k}^-, n+1} + \omega(\widehat{\Omega}_n, e^{-x_j}) \widetilde{A}_{j, n+1}. \end{aligned}$$

The first boundary condition corresponds to $x = x_0$, the second to $c = 0$, and the last to $c = 32$ where \overline{k} is the index between 0 and K such that $c_{\overline{k}}$ is as close to 32 as possible [3]. Next, equation (9) for cells in Ω^* is discretized as

$$\widetilde{\Omega}_{j, n+1}^* = \widetilde{\Omega}_{j, n}^* - \lambda_x \rho_d (\widetilde{\Omega}_{j, n}^* - \widetilde{\Omega}_{j-1, n}^*) + \begin{cases} 0, & x_j \in X_a, \\ -(\Delta t) \alpha(\widehat{A}_n, e^{-x_j}) \widetilde{\Omega}_{j, n}^*, & x_j \in X_b. \end{cases}$$

The boundary condition given by the fourth and fifth lines of (10) become

$$\begin{aligned} \widetilde{\Omega}_{0, n+1}^* &= \Delta t \frac{\omega(\widehat{\Omega}_n, e^{-x_0})}{\rho_d} \widetilde{A}_n^* \\ \widetilde{\Omega}_{j^+, n+1}^* &= 2\widetilde{\Omega}_{j^-, n+1}^*. \end{aligned}$$

For the differentiated cells, the grid points for the time domain is the same as stated above. The grid points for the age domains $[0, 480]$ and $[0, 192]$ for precursor and mature cells respectively, are given by $s_i = i\Delta s$ where $\Delta s = 1/w$ for some integer w and $i = 1, \dots, I_m, \dots, I_p$. Note that \tilde{P} and \tilde{M} represent the numerical approximations to P and M , respectively. An explicit upwind scheme is used to approximate equations (11) and (13) as

$$\begin{aligned} \tilde{P}_{i, n+1} &= \tilde{P}_{i, n} - \lambda_s (\tilde{P}_{i, n} - \tilde{P}_{i-1, n}) \\ \tilde{M}_{i, n+1} &= \tilde{M}_{i, n} - \lambda_s (\tilde{M}_{i, n} - \tilde{M}_{i-1, n}) \end{aligned}$$

The boundary conditions are given as

$$\begin{cases} \tilde{P}_{0, n} = \rho_d (\mathcal{T}_c(\widetilde{\Omega}_{j, -, n}) + \widetilde{\Omega}_{j, n}^*) \\ \tilde{P}_{v w^+, n} = 2\tilde{P}_{v w^-, n} \\ \tilde{M}_{0, n} = 2\tilde{P}_{I_p, n} \end{cases} \quad \text{for } v = 24, 48, 72, \dots, 456$$

The numerical approximations for leukemic cells are derived similarly. This numerical method is a first-order method. Extensions of the scheme in higher-order can be considered as a follow-up project.

3 Implementation

All three models were implemented in Matlab R2015b. Simulations were run on an ASUS Notebook with a 2.4 GHz Intel Core i5 processor and 8 GB of RAM.

The complete simulation for this project involves three steps: steady state, CML genesis, and treatment. For the first step, a small number of healthy cells are simulated by looping over time until a steady mature cell count is reached. The model is initialized by setting $\Omega_{0,32}^-(0) = 1$, or some other small number. Although the results are not dependent on the initial condition, choosing a cycling stem cell with maximum affinity at hour 32 of the cell cycle guarantees that the system will have two cycling stem cells 17 discrete time steps later when the cell completes mitosis. Steady state is reached at around two years when there are approximately 6.58×10^{10} mature Ph^- cells. The steady state profile for Ph^- cells is used as the starting value for Ph^- cells when CML genesis begins. The Ph^+ population is initialized by setting $\Omega_{0,32}^+(0) = 1$, or some other small number. The duration of CML genesis is assumed to be 15 years for these simulations. At this point, most runs predict the Ph^+ population to be roughly 99.5% of the total cell population. Lastly, treatment is simulated using the Ph^- and Ph^+ population values from CML genesis as starting values. The $\text{Ph}^{+/A}$ initial population will be set during the first time step to be $\Omega_{k,c}^{+/A}(0) = \Omega_{k,c}^{+/I}(0)$. Treatment was simulated for 400 days for validation. Other lengths of treatment were explored during testing.

3.1 Agent Based Model

Each stem cell in the Agent Based Model is represented and tracked using a row vector whose entries hold the values for affinity and cell cycle position. Additional values were added during testing to track transition characteristics. Row vectors tracking Alpha stem cells are grouped in a matrix A, so that transitions to these cells can be executed simultaneously and efficiently with built-in Matlab functions. Similarly, Omega stem cells are grouped into a matrix O. When a single stem cell moves between compartments, the row of the matrix corresponding to the cell is deleted from one matrix and inserted at the end of the other. Implementing the ABM in this way reflects the stochastic nature of the stem cell transitions in this model, but is quite inefficient as matrix sizes will change on each iteration.

Differentiated cells in the ABM are not stochastic in nature. Because of this, precursor and mature cells need not be simulated individually. These cells can be represented as a single vector whose entries hold the total number of differentiated cells with the same cell age. At each time step, the total number of Omega cells that have reached minimum affinity will be used to set the first entry of the differentiated cell vector. In this way, the ABM is updated similarly to the difference equations.

Time steps of one hour were used for all simulations.

3.2 Difference Equations

At each time step, approximately 10^5 simple equations are computed. The difference equations were vectorized to achieve a more efficient simulation of these computations. A and B are represented as column vectors, where the k^{th} entry contains the number of cells with an affinity level of k . Ω and Ψ cells are dependent on both affinity and cell cycle. These cells are tracked by matrices whose (k, c) entries contain the number of cells with affinity k , at position c in the cell cycle. P and M are structured as column vectors whose j^{th} entry contains the number of cells of age j in the respective compartment. Time steps of one hour were used for each phase of simulation.

3.3 PDE

Like the ABM and difference equation models, the PDE model was implemented to take advantage of many of Matlab's built in matrix functions and capabilities. The cells in A^* are tracked by a single number, since these cells are only dependent on real time t . Cells in A , Ω^* , P and M are all dependent on two of the four variables. They are represented by vectors of size dependent on the mesh size being used. For A and Ω^* , the j^{th} entry in the representative vector holds the number of cells with affinity level x_j . For P and M , the i^{th} entry in the representative vector contains the number of cells at age s_i . The number of Ω cells with affinity x_j at cell cycle position c_k are tracked by the (j, k) entry of a matrix whose size is dependent on the mesh sizes for x and c domains.

The mesh sizes used for validation are consistent with those given in [3] and can be found in table B.2. Due to the long 15 year simulation of CML Genesis, a much coarser mesh was used for this phase of model simulation. After healthy cell steady state simulation is complete A , Ω , Ω^* , P and M are restricted to the coarse domain. These values are then used as initial populations for Ph^- cells during CML genesis.

4 Validation

4.1 ABM

The complexity of the ABM is based on the number of agents in the system. The completed model was validated by running simulations first on a small number of cells, increasing gradually to larger values. Validity was determined by comparing resulting cell counts and figures to those presented by Kim *et al* and to the difference equation model, which was implemented and validated before the ABM. Furthermore, the ability to simulate total stem cell counts on the order of 10^5 or larger will demonstrate an efficient implementation of the ABM. Simulations of the nonleukemic cell population were run and validated before introducing the algorithm alterations representing CML genesis and Imatinib treatment.

Due to the stochastic nature of the ABM, each run of the model produces slightly different results. However, the general characteristics of each figure produced by each run should be similar and comparable to each other as well as to the validation figures. Two such runs of steady state simulations can be seen in figure 3. It is clear that each of these runs showcases the desired characteristics of healthy stem cells in a steady state population. A general upward stepping pattern is seen in Omega stem cells as affinity decreases. There is a large accumulation of Alpha stem cells at the maximum affinity level. The total number of stem cells for these simulations also validates this model. The number of Ph^- stem cells at steady state is on the order of 10^6 , which is in accordance with the Roeder model. There are 91,379 cells and 91,452 cells with maximum affinity in the top and middle images of figure 3, respectively. This is around the number of cells produced by the difference equation model (fig. 3).

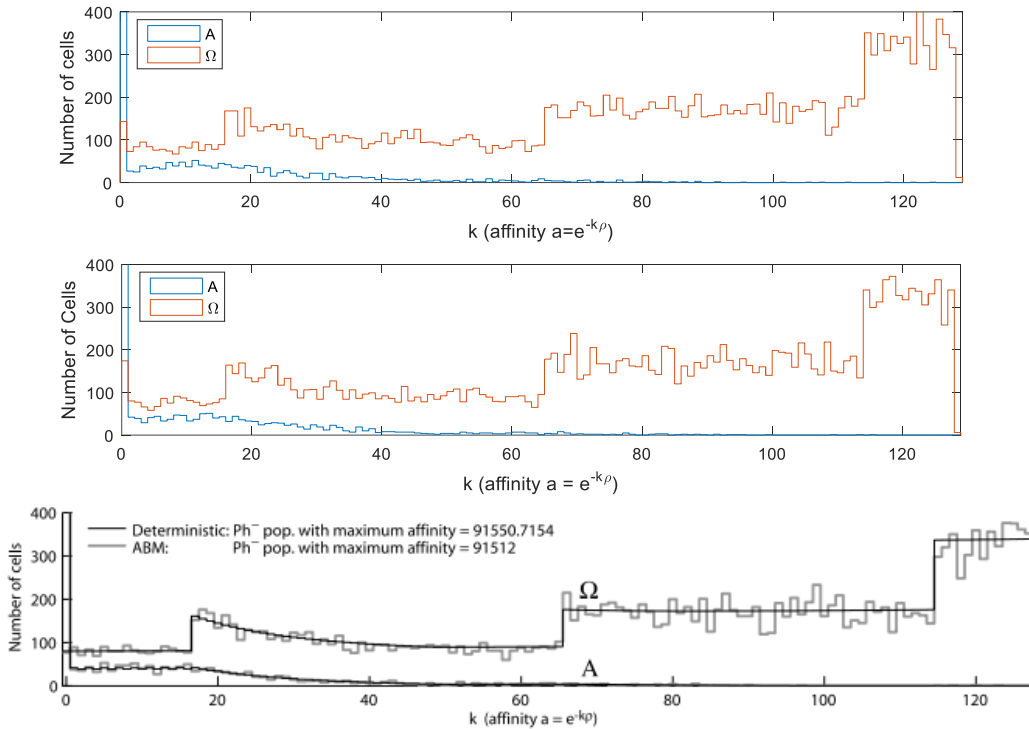


Figure 3: Steady state profile for nonleukemic stem cells achieved by ABM. Both resting and proliferating stem cell populations are shown. The figures shown on top and in the middle are two separate runs of steady state simulation using ABM. The original figure from [2], shown on bottom, shows desired results of an ABM run in gray.

Validation of ABM CML genesis is shown in figure 4. The two images here represent two separate runs CML genesis resulting from the same steady state profile. Total mature cell counts for Ph^- and Ph^+ cells are plotted over time. These simulations are overlaid onto the validation images. Depending on the run, it can be seen that the ABM predicts different rates of cancer development, but it general similar trends are seen between runs and the validation image.

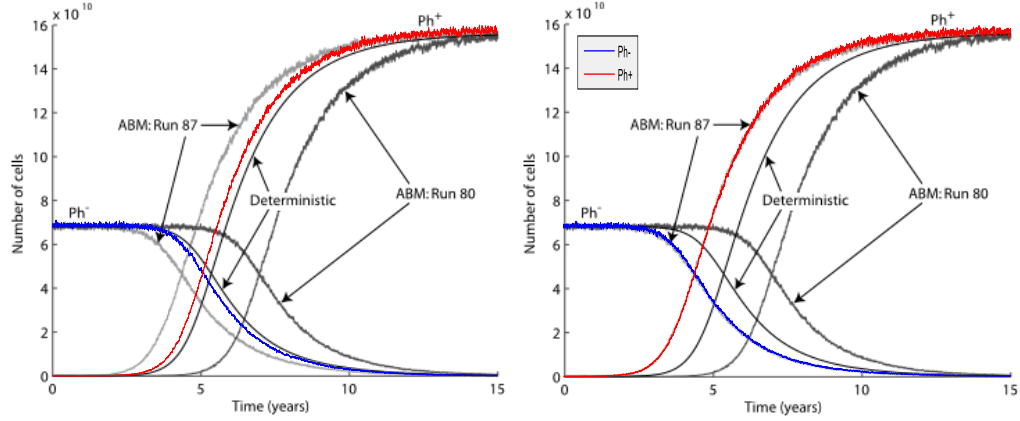


Figure 4: Simulation of CML genesis by two separate runs of ABM. Dynamics of both leukemic (Ph^+) and nonleukemic (Ph^-) cells are shown by plotting the number of mature cells in each population versus time. The original figure from [2] shown in gray is overlaid with the results from this project. Ph^- cells are plotted in blue. Ph^+ cells are plotted in red.

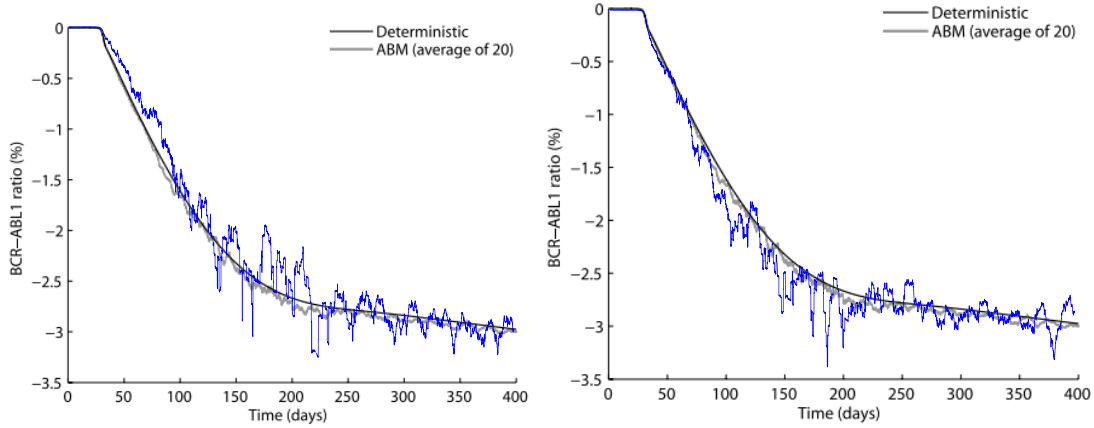


Figure 5: BCR-ABL1 ratio during Imatinib treatment. The original figure from [2] shown in gray is overlaid with the results from this project in blue. Two separate runs of ABM are shown.

Lastly, the treatment stage of simulation was validated using the BCR-ABL1 ratio. This ratio provides a measure of the ratio of CML cells to healthy cells. It is calculated using the formula given in Roeder *et al.*:

$$BCR - ABL1 \text{ ratio} = \frac{\# \text{ mature } Ph^+ \text{ cells}}{\# \text{ mature } Ph^+ \text{ cells} + 2 * \# \text{ mature } Ph^- \text{ cells}} \quad (15)$$

The number of mature Ph^+ cells used here is the total number of leukemic cells, both affected and unaffected. Due to the stochastic nature of the model, each individual run results in a very jagged curve. Despite this noise, the biphasic decline that is characteristic of Imatinib treatment is captured by this simulation. Thus, this model is fully validated.

4.2 Difference Equations

Validation of the difference equation model was achieved by recreating the figures presented in Kim *et al.* The results of simulation were overlaid onto the figures from [2] to determine if the figure was accurately recovered. Initially, Matlab's *binornd(N,P)* function was used to calculate $B_k(t)$ and $\Psi_{k,c}(t)$. This produced the results seen in figure 6. It can be seen that the desired dynamics are present, namely an accumulation of A cells at $k = 0$ which then tapers to zero around $k = 60$. To achieve smooth curves that exactly replicate the desired figure, all binomial distributions were replaced with their respective expected values.

Validation of this model's steady state is shown in figure 7. The steady state profile of nonleukemic stem cells for the difference equations is achieved by plotting $A_k(t_{ss})$ and $\sum_c \Omega_{k,c}(t_{ss})$ versus affinity level k , where t_{ss} is the steady state time. The blue and red curves produced during simulation closely match the curves from [2]. Slight variations can be seen at the jumps in Ω that occur near $k = 15, 65, 115$. Overall, this simulation is considered successful.

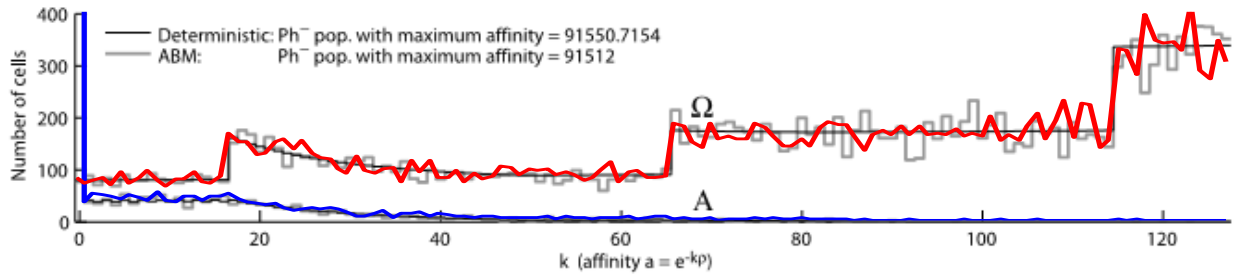


Figure 6: Steady state profile for nonleukemic stem cells achieved by ABM and difference equation method. Both resting and proliferating stem cell populations are shown. The original figure from [2] shown in gray, is overlaid with the results from this project. The blue line shows the number of resting stem cells while red plots the number of cycling stem cells. Binomial distribution used for B_k and $\Psi_{k,c}$.

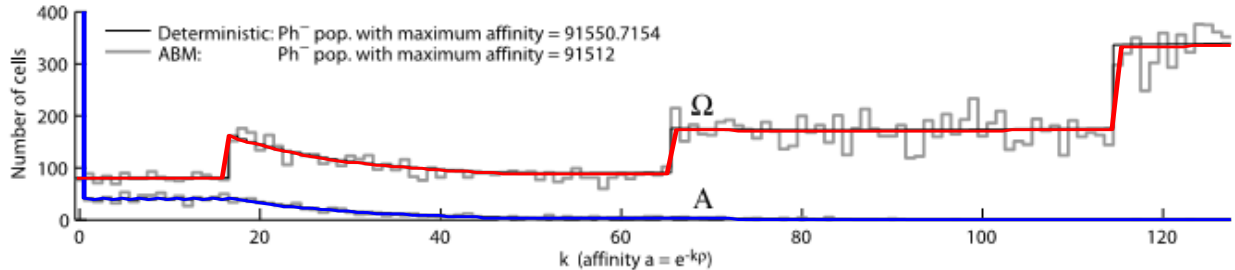


Figure 7: Steady state profile for nonleukemic stem cells achieved by ABM and difference equation method. Both resting and proliferating stem cell populations are shown. The original figure from [2] shown in gray, is overlaid with the results from this project. The blue line shows the number of resting stem cells while red plots the number of cycling stem cells. Expected value for B_k and $\Psi_{k,c}$ used instead of binomial distributions.

Figure 8 depicts the number of mature leukemic ($M^+(t) = \sum_s M_s^+(t)$) and nonleukemic cells ($M^-(t) = \sum_s M_s^-(t)$) versus time. As expected, simulation of Ph^- cells begin at a steady state value of approximately 6.58×10^{10} cells and begin to decrease to zero just before five years. Beginning at the same time point, the Ph^+ population begins to sharply increase until it

approaches a cell count of 16×10^{10} cells. This is consistent with the original model and therefore successfully validates CML genesis for this model.

Simulation of treatment is again validated using the BCR – ABL ratio. The biphasic decline in the BCR-ABL1 ratio that can be seen in blue (fig. 9) is consistent with the original figure from [2] and validates this implementation.

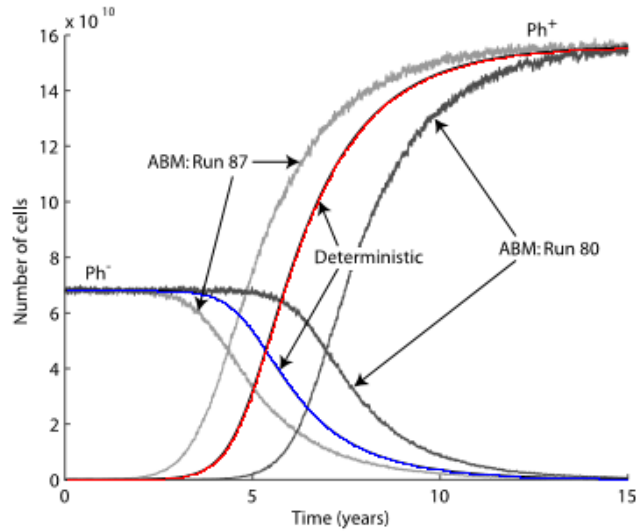


Figure 8: Simulation of CML genesis. Dynamics of both leukemic (Ph⁺) and nonleukemic (Ph⁻) cells are shown by plotting the number of mature cells in each population versus time. The original figure from [2] shown in gray is overlaid with the results from this project. Ph⁻ cells are plotted in blue. Ph⁺ cells are plotted in red.

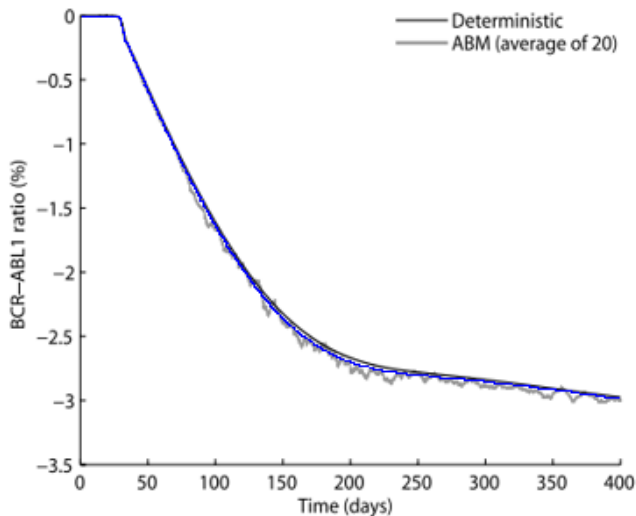


Figure 9: BCR-ABL1 ratio during Imatinib treatment. The original figure from [2] shown in gray is overlaid with the results from this project in blue.

4.3 PDE

Validation of the PDE model is accomplished in a slightly different manner. The goal is to recreate the figures presented in Kim *et al* for each phase of simulation. Before this can be done, the numerical approximation for each compartment is verified by comparing the PDE output to the difference equation output. The numerical approximations for P and M, the simplest of the equations, were verified first by initializing the system with a small amount of precursor cells and simulating cell development for various time periods (5, 20 and 30 days). This simulation does not involve the stem cell equations as they are initialized with zero cells. The total amount of precursor and mature cells after these durations were compared to the difference equation output and were verified to be identical, thereby justifying the validity of the P and M numerical approximations.

Next, the numerical approximations for Alpha and Omega cells were implemented and verified. To determine that updates within each compartment were accurate, the transition probabilities ω and α were set to zero to prevent cells transferring between the two compartments. Various initial populations of Alpha and Omega were used to determine that total cell counts remained constant away from the boundaries. Transitions from Omega to Alpha were verified by setting ω to zero. This allows Omega cells to transition to Alpha but prevents them from transitioning back to Omega. It can then be determined if equal amounts of cells are leaving Omega and entering Alpha at each time step. Validation of the Alpha to Omega transition was completed similarly.

Validation is concluded with numerical simulations of the entire system, resulting in figures similar to those presented by Kim *et al*. Validity ideally is determined by overlaying this model's output onto the images in [3] to demonstrate the ability of the PDE model to capture CML behavior (fig. 10, 11).

In examining the steady state profile of stem cells (fig. 10), the PDE model seems to underestimate the number of cells at each level of affinity for both Alpha and Omega stem cells. However, the general shape of the profile appears to be consistent with the desired outcome. This would suggest that the overall structure of the code is correct and the differences between the figures can be accounted for by a scaling error, which is yet to be found.

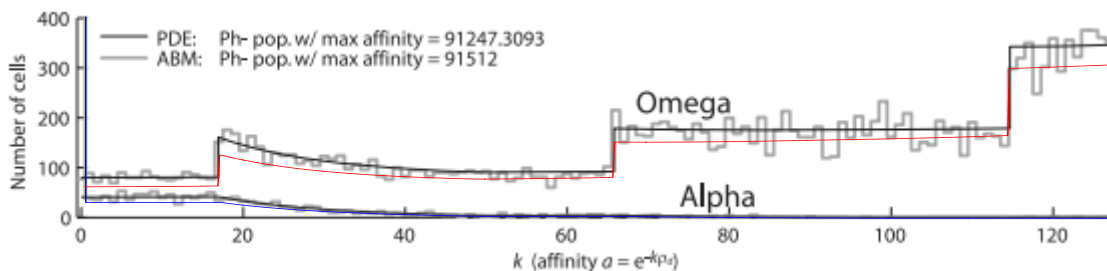


Figure 10: Steady state profile of nonleukemic cell population achieved by ABM and PDE model. Both resting and proliferating stem cell populations are shown. The original figure from [3] shown in gray. Results from this project overlaid in blue (Alpha cells) and red (Omega cells).

Plots of CML genesis and treatment were not overlaid onto validation images for the PDE model, since it was clear that they are not exact matches. While this implementation of the PDE model does predict CML genesis will occur, the behavior of the mature cell populations over time does not follow the behavior seen in the validation image. Almost immediately after CML simulation begins, the Ph^+ population reaches its steady state level and the Ph^- population instantaneously declines to nearly zero. The source of this error is not yet determined.

Simulation of the treatment phase with the PDE model yielded mixed results. While the resulting image did not agree with the validation image, the characteristic biphasic decline of Imatinib treatment can be seen (fig. 12). The minimum BCR – ABL ratio attained by this implementation is 0.06%, which is much lower than the BCR – ABL ratio reported in Kim *et al.* (approximately 8.2%). The appearance of biphasic decline suggests that, like the steady state simulation, the underlying structure is correct. It is possible that the error in CML genesis simulation is the cause of the differences seen here.

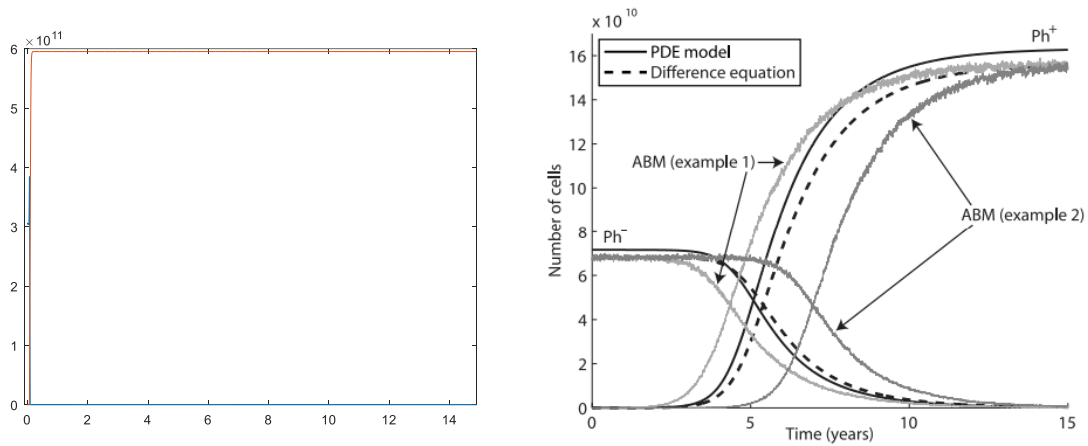


Figure 11: CML genesis as simulated by each of the three models. Dynamics of both leukemic (Ph^+) and nonleukemic (Ph^-) cells are shown by plotting the number of mature cells in each population versus time. Validation image from [3] on the right. Results from this project on the left.

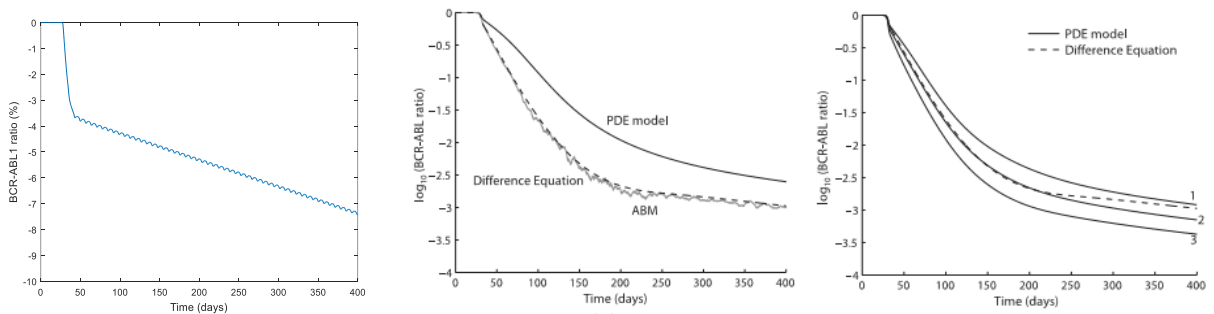


Figure 12: The log of the BCR-ABL ratio (15) is plotted over the 400 day treatment simulation. Results from [3] are shown in the images in the center and right. The figure on the left are the results of this project. The figure in the center shows difference between the PDE model and the two discrete model when the original values of $r_{inh}=0.05$ and $r_{deg}=0.033$ are used. The figure on the right demonstrates that the PDE model achieves more similar results these parameters are varied; $(r_{inh}, r_{deg}) = (0.1, 0.037), (0.1, 0.04),$ and $(0.1, 0.43)$ for cases 1, 2 and 3 respectively.

5 Complexity Analysis and Model Comparison

As shown in section 4, the three models implemented in this project produce reasonably similar simulations of each cell population and compartment. However, the models greatly differ in terms of efficiency. The ABM can become quite computationally complex, as it is based on the number of stem cells being simulated. At initial implementation by Roeder in 2006, simulations of approximately 10^5 stem cells were achieved. This is only about $\frac{1}{10}$ of realistic values. In this implementation, approximately 10^6 stem cells were simulated.

The system of difference equations model was created to combat this computational complexity and create a much more efficient model. Simulation of the difference equations requires computing tens of thousands of fairly simple equations at each time step, however this method proves to be much more efficient than the ABM as demonstrated by the average run times reported in table 1. While the PDE model is grouping cells by their common characteristics similarly to the difference equations, it is not as efficient for each phase of the simulation due to smaller time steps. This is especially noted for simulation of the healthy cell steady state population which uses a time step that is one tenth of the time step for the discrete model.

Average Run Time	ABM	Difference Equations	PDE
Steady State (2 yrs)	44.4919 s	2.5857 s	32.983 min (dt=0.1)
CML Genesis (15 yrs)	14.06 min	45.606 s	4.7836 min (dt=0.5)
Treatment (400 days)	38.5801 s	5.4113 s	33.6282 s (dt=0.45)

Table 1: Average run times for each phase of simulation. Shown are the averages for 20 runs of each model. The same steady state profile was used as an initial population for each of the 20 ABM runs of CML genesis and treatment simulations.

It is clear from these values that the difference equations are significantly faster than both the ABM and PDE models. Surprisingly, the PDE model is significantly slower than either of the other two when simulating the steady state population. In comparison to the original run times for each model, these implementations appear to be much more efficient. Run times for CML genesis, the longest simulation phase, were reported to be 6.5 hours, 4.5 minutes and just under 2 hours for the ABM, difference equations and PDE model respectively [3].

6 Testing

There are many questions we would like to be able to answer about CML and Imatinib treatment using these models. Firstly, it has been shown that due to its stochastic nature, the ABM produces different output on each run. Is there a chance that the ABM will not predict the development of cancer? How does the average run of the ABM compare to the deterministic difference equations? What is the average duration for CML genesis?

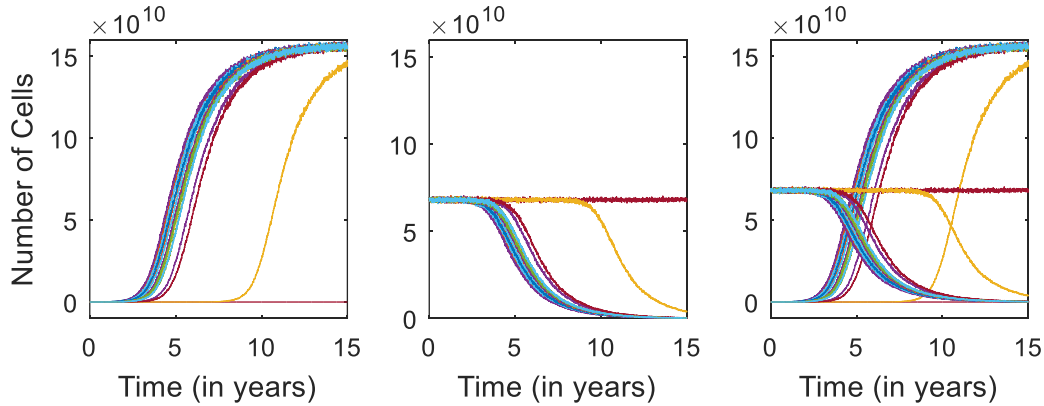


Figure 13: Mature cell populations for Ph^+ (left) and Ph^- (left) during 15 year simulation of CML genesis for 20 different runs of the ABM. Figure on right shows Ph^- and Ph^+ plotted together over time.

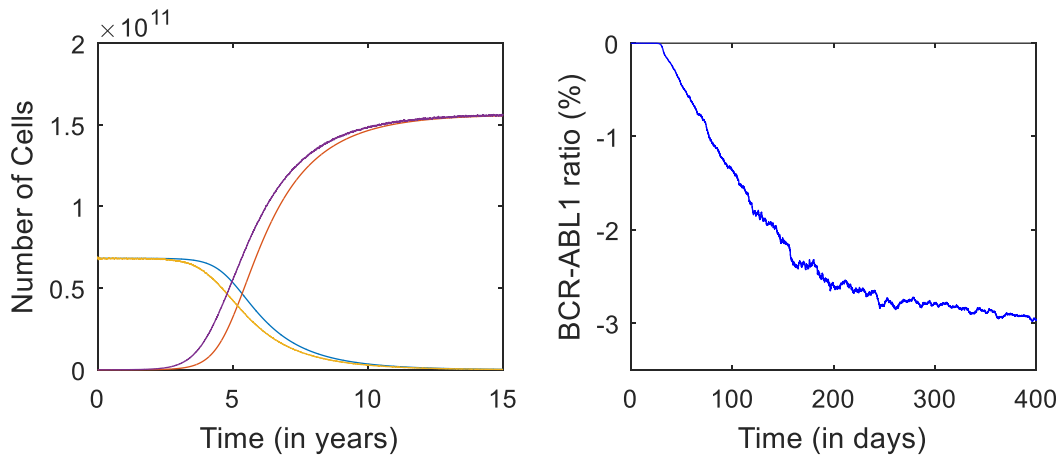


Figure 14: Average of 18* ABM runs plotted over time for CML genesis (left) and treatment (right). The plot on the right shows the ABM average (yellow and purple) versus the difference equations (red and blue). *Only runs that attained a 99% BCR – ABL barrier were used to calculate the average.

It can be seen from figure 13 that the ABM does not always predict the development of CML within a 15 year period. Of the 20 runs simulated, 18 of them reached the desired 99% BCR – ABL threshold. One of the two simulations that did not meet this barrier within the 15 year simulation period does show the development of CML (in yellow), but at a much slower rate. This simulation predicts that the 50% threshold will be met at the 10 year mark, which is almost double the time the average run takes (table 2). The last of the 20 simulations fails to reach even the 20% threshold (in dark red). It predicts extinction of the Ph^+ population by day 116 of simulation.

An average of the 18 runs that met the 99% BCR – ABL barrier shows behavior almost identical to a single run of the difference equation model (fig. 14). It seems as though the ABM is predicting CML development at a slightly faster pace than the difference equations. This is further demonstrated in the average time to reach thresholds of 20%, 50% and 99% (table 2). There is reason to believe that an average over a larger sample of runs would match more closely

with the difference equation model. However, this hypothesis was not fully explored in the timeframe of this project.

Threshold Met Time	ABM	Difference Equations
BCR – ABL = 20%	4.3505 years	4.8825 years
BCR – ABL = 50%	5.3573 years	5.900 years
BCR – ABL = 99%	12.1705 years	12.8840 years

Table 2: Simulation time at which BCR –ABL ratio thresholds were met. Shown are the averages for 18* runs of the ABM. The same steady state profile was used as an initial population for each of the 18 ABM runs of CML genesis. *Only runs that attained a 99% BCR – ABL barrier were used to calculate the average.

It is also beneficial to explore what these models can tell us about the effects of Imatinib. Over the first 400 days of treatment, all three models predict a biphasic decline in the BCR – ABL ratio. What does this mean in terms of the Ph⁻ and Ph⁺ cells populations and what will happen over an extended treatment period? Does a steady state arise? Imatinib is an effective control for CML, but it is not a cure. The majority of CML patients will rely on Imatinib or a similar drug for the rest of their lives or risk recurrence of the disease. Do these models demonstrate this outcome? These questions were addressed using the difference equation model due to its efficient nature; similar results would be expected when using the ABM and PDE models.

As previously shown, the treatment phase of simulation results in a biphasic decline in the BCR – ABL ratio. Figure 15 shows what this means in terms of the mature Ph⁻ and Ph⁺ cell populations. At the beginning of treatment, the number of leukemic cells in the system rapidly declines to levels that appear close to zero. After closely examining this time frame, it can be seen that while there is a drastic downsize in the population, CML is not completely eradicated. The Ph⁺ population reaches a minimum value of approximately 5.6×10^6 cells after 160 days of treatment.

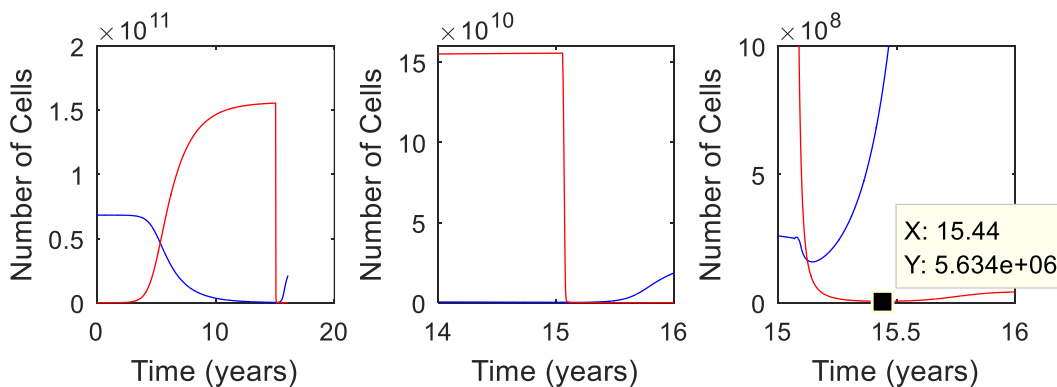


Figure 15: Mature cell populations for Ph⁻ (blue) and Ph⁺ (red) during 15 year simulation of CML genesis and 400 day treatment simulation.

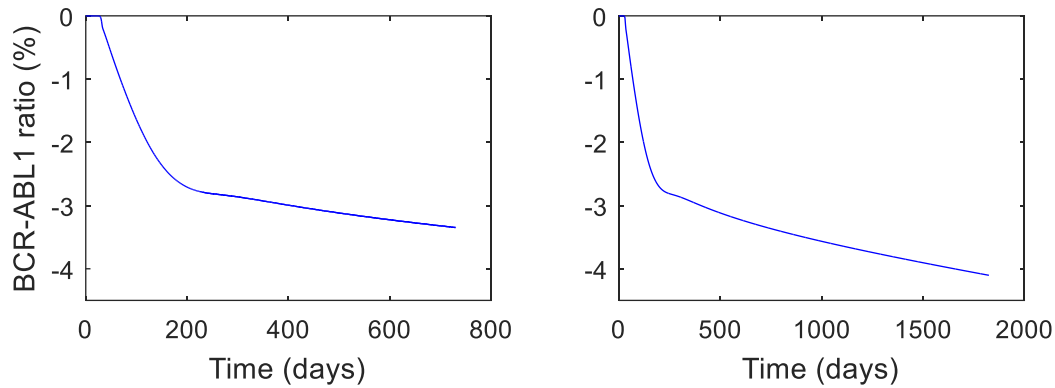


Figure 16: Simulations of extended treatment. The log of the BCR – ABL ratio is plotted over the duration of treatment. Treatment is simulated for 2 years (left) and 5 years (right).

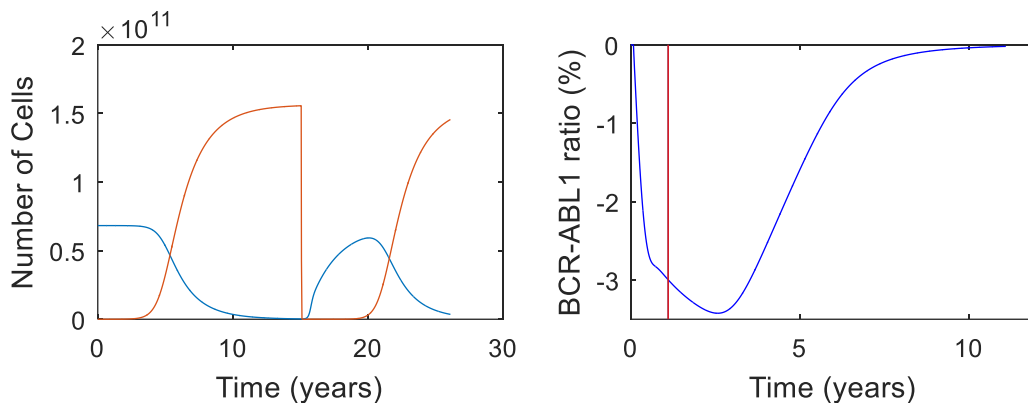


Figure 17: Recurrence of CML when treatment is stopped. Mature Ph⁻ (blue) and Ph⁺ (red) cell populations over the 15 year CML genesis phase, 400 days of treatment and 10 years post treatment are plotted on the left. Log of the BCR – ABL ratio is plotted in blue on the right. The red line indicates the time at which treatment ends.

If treatment were to be extended past the 400 days, could this population be completely eradicated? Simulations of 2 years and 5 years were run to address this question. The results suggest that the BCR-ABL ratio will continue to decline steadily over time (fig. 16). It does not seem that a steady state will be reached, suggesting that it would be possible to eradicate the Ph⁺ cell population if the duration of treatment is long enough. However, this does not agree with the true behavior of CML in actual patients. This presents a possible weakness in the model.

Figure 17 can be used to predict what happens post treatment. Here treatment is considered to be 400 days long, after which point treatment will cease to be simulated and all populations will transition according to the original transition rules. It can be seen that approximately 5 years post-treatment, the Ph⁺ population has overgrown the Ph⁻ population. By 10 years post-treatment, the BCR-ABL ratio has reached the 99% barrier once more, suggesting a recurrence of CML.

7 Conclusion

At completion of this project all three models have been implemented and simulate the growth and development of both healthy and leukemic cells according to the rules and assumptions set forth in the cell state diagram (fig. 1). The agent based model realistically simulates each stem cell individually. The stochastic nature of this model is more applicable to authentic biological concepts. However, it is not the most efficient model which can make it somewhat cumbersome to use for testing. The difference equation model is able to capture an average simulation of the ABM in a very efficient manner. It is therefore the easiest to use for testing and validation as it produces quick and consistent results. The PDE model turned out to be the least efficient model implemented for this project. It is the only continuous time model, which better correlates to real life cell growth and development. It is perhaps the best of the three models to use to explore parameter sensitivity, especially in relation to step sizes and the parameters involved in treatment (r_{inh} , r_{deg}) as demonstrated in figure 12. However, its slow computation time may make it cumbersome to use in extensive testing.

Further exploration of these models could include altering the underlying structure of the model to more accurately reflect true biological behavior of hematopoietic cells. This could include: allowing variation in the fixed parameters for cell lifespan and cell cycle clock duration, relaxing the condition on symmetric cellular division, and addressing discrepancies between simulated treatment and clinical results of treatment.

Appendix A: Project schedule

The project is divided into four phases:

Phase 1: October – Early December

- Implement difference equation model
- Improve efficiency and validate

Phase 2: January – Early March

- Implement Agent Based Model
- Improve efficiency and validate

Phase 3: March – Early April

- Implement basic PDE method
- Validate for precursor and mature populations

Phase 4: mid-February – April

- Implement numerical approximations for stem cell compartments
- Testing and model comparison
- Draw conclusions

Appendix B: Parameter estimates

The sigmoidal transition functions given by Roeder *et al.* take the form

$$f_{\alpha/\omega}(A/\Omega(t)) = \frac{1}{v_1 + v_2 \exp\left(\frac{v_3 A/\Omega(t)}{\tilde{N}_{A/\Omega}}\right)} + v_4 \quad (\text{B.1})$$

where

$$\begin{aligned} v_1 &= \frac{h_1 h_3 - h_2^2}{h_1 + h_3 - 2h_2}, \\ v_2 &= h_1 - v_1, \\ v_3 &= \ln\left(\frac{h_3 - v_1}{v_2}\right), \\ v_4 &= f_{\frac{\alpha}{\omega}}(\infty), \end{aligned}$$

and

$$\begin{aligned} h_1 &= \frac{1}{f_{\alpha/\omega}(0) - f_{\alpha/\omega}(\infty)}, \\ h_2 &= \frac{1}{f_{\alpha/\omega}\left(\frac{\tilde{N}_A}{2}\right) - f_{\alpha/\omega}(\infty)}, \\ h_3 &= \frac{1}{f_{\alpha/\omega}(\tilde{N}_A) - f_{\alpha/\omega}(\infty)}. \end{aligned}$$

The parameter values for $f_{\alpha/\omega}(\ast)$ for each cell type are as given by Roeder *et al.* and can be found in the Table 1 with all other parameter values.

Table B.1 Parameters

Parameter	Description	Ph ⁻	Ph ⁺ /Imatinib-affected
a_{\min}	Min value of affinity a	0.002	0.002
a_{\max}	Max value of affinity a	1.0	1.0
$f_{\alpha}(0)$	Transition characteristic for f_{α}	0.5	1.0
$f_{\alpha}(\tilde{N}_A/2)$	Transition characteristic for f_{α}	0.45	0.9
$f_{\alpha}(\tilde{N}_A)$	Transition characteristic for f_{α}	0.05	0.058
$f_{\alpha}(\infty)$	Transition characteristic for f_{α}	0.0	0.0
\tilde{N}_A	Scaling factor for f_{α}	10^5	10^5
$f_{\omega}(0)$	Transition characteristic for f_{ω}	0.5	1.0/0.0500
$f_{\omega}(\tilde{N}_{\Omega}/2)$	Transition characteristic for f_{ω}	0.3	0.99/0.0499
$f_{\omega}(\tilde{N}_{\Omega})$	Transition characteristic for f_{ω}	0.1	0.98/0.0498
$f_{\omega}(\infty)$	Transition characteristic for f_{ω}	0.0	0.96/0.0496
\tilde{N}_{Ω}	Scaling factor for f_{ω}	10^5	10^5
r_{inh}	Inhibition intensity		0.050
r_{deg}	Degredation intensity		0.033

Table B.2 Mesh Sizes for PDE Numerical Approximations

Mesh Size	Steady State	CML Genesis	Treatment
Δt	0.1	0.5	0.45
Δx	$2\rho_d \cdot \Delta t$	ρ_d	ρ_d
Δc	0.2	1	1
Δs	0.1	0.5	0.5

References

- [1] Roeder, I., Horn, M., Glauche, I., Hochhaus, A., Mueller, M.C., Loeffler, M., 2006. Dynamic modeling of imatinib-treated chronic myeloid leukemia: functional insights and clinical implications. *Nature Medicine*. 12(10): pp. 1181-1184
- [2] Kim, P.S., Lee P.P., and Levy, D., 2008. Modeling imatinib-treated chronic myelogenous leukemia: reducing the complexity of agent-based models. *Bulletin of Mathematical Biology*. 70(3): pp. 728-744.
- [3] Kim, P.S., Lee P.P., and Levy, D., 2008. A PDE model for imatinib-treated chronic myelogenous leukemia. *Bulletin of Mathematical Biology*. 70: pp. 1994-2016.

[4] National Cancer Institute: PDQ® Chronic Myelogenous Leukemia Treatment. Bethesda, MD: National Cancer Institute. Date last modified 9/21/2015. Available at: <http://www.cancer.gov/types/leukemia/patient/cml-treatment-pdq>.